

# High-Fidelity Transfer of Functional Priors for Wide Bayesian Neural Networks by Learning Activations

**Marcin Sendera\***  
 Jagiellonian University  
 Mila, Université de Montréal

**Amin Sorkhei**

**Tomasz Kuśmierczyk\***  
 Jagiellonian University

## Abstract

Function-space priors in Bayesian Neural Networks provide a more intuitive approach to embedding beliefs directly into the model’s output, thereby enhancing regularization, uncertainty quantification, and risk-aware decision-making. However, imposing function-space priors on BNNs is challenging. We address this task through optimization techniques that explore how trainable activations can accommodate complex priors and match intricate target function distributions. We discuss critical learning challenges, including identifiability, loss construction, and symmetries that arise in this context. Furthermore, we enable evidence maximization to facilitate model selection by conditioning the functional priors on additional hyperparameters. Our empirical findings demonstrate that even BNNs with a single wide hidden layer, when equipped with these adaptive trainable activations and conditioning strategies, can effectively achieve high-fidelity function-space priors, providing a robust and flexible framework for enhancing Bayesian neural network performance. Our code is made public at ([github](#)).

## 1 INTRODUCTION

Models trained in a function-space rather than in the space of weights and biases (parameters space) exhibit flatter minima, better generalization, and improved robustness to overfitting (Qiu et al., 2024). Better properties achieved by focusing directly on the output space are particularly advantageous in scenarios where

the relationship between parameters and function behavior is not straightforward, especially for Bayesian Neural Networks (BNNs). In particular, function-space priors offer a better method of specifying beliefs on data modeled by a model, rather than just the parameters, leading to the intuitive and often more meaningful representation of prior knowledge (Tran et al., 2022; Sun et al., 2019).

Function-space priors can be conveniently specified in terms of Gaussian Processes (GPs). Instead of directly specifying complex distributions over model parameters, GPs allow for defining priors over entire functions, capturing smoothness, periodicity, or other functional properties through the choice of kernel. This enables the model to work across various input spaces and offers interpretable uncertainty quantification.

Finding a GP that matches a wide BNN is straightforward. A classic result by Neal (1996); Williams (1996), later extended to deep NNs by Lee et al. (2017); Matthews et al. (2018), shows that wide layers in NNs behave *a priori* like GPs (networks exhibit such properties already at width  $\approx 100$ , which means, most modern networks are wide, at least partially) by identifying the kernel of a GP that matches covariance of a (B)NN. On the other hand, finding BNNs that exhibit the desired behavior of GPs is a notoriously difficult problem, with analytical solutions existing for only a few GP kernels. For example, Meronen et al. (2020) found a solution (a BNN’s activation function) for the popular Matern kernel by employing Wiener-Khinchin theorem. To address the challenge of imposing function-space *a priori* behavior to BNNs, Flam-Shepherd et al. (2017), Flam-Shepherd et al. (2018), and especially Tran et al. (2022), attempted to find appropriate priors on parameters with gradient-based optimization. Their approach requires deep networks equipped with complex distributions and additionally presents an undisclosed challenge in learning posteriors.

In this work, we demonstrate that by learning activations in addition to priors on weights and biases, we can

Preprint.

\* denotes equal contribution

contact: [marcin.sendera@{uj.edu.pl, mila.quebec}](mailto:marcin.sendera@{uj.edu.pl, mila.quebec})

achieve faithful function-space priors using just shallow BNNs. We establish a practical and straightforward alternative to finding closed-form solutions for activations to impose function-space priors on BNNs. Our method involves transferring priors from GPs to BNNs by aligning the covariance induced by the BNN with the desired GP kernel. This is achieved by optimizing the distributions of the weights, biases, and activations within the BNN, using gradient-based methods. Additionally, we leverage hypernetworks to condition the priors on GP hyperparameters, ensuring that the BNN can faithfully mimic the desired GP’s properties e.g. allow for marginal likelihood optimization and model selection. Our approach relies on an efficient variant of the Wasserstein distance for the optimization loss. Although the method is described in terms of GP priors as targets, it is general and can be applied for arbitrary functional priors, making it a versatile tool for enhancing BNNs.

Our contributions are as follows: (1) we introduce a practical approach for imposing GP-like function-space priors on BNNs; to the best of our knowledge, we are the very first considering learning activations in this setting; (2) we employ hypernetworks to condition these priors on, e.g., GP hyperparameters, and (3) we demonstrate empirically that even shallow BNNs can achieve high-fidelity function-space priors through this method, providing an alternative to complex deep models.

## 2 PRELIMINARIES

**On convergence of wide BNNs to GPs.** Behavior akin to GPs has been identified in wide neural networks with a single hidden layer by Neal (1996); Williams (1996) and later generalized for deep architectures by Lee et al. (2017); Matthews et al. (2018) who considered stacking multiple such the wide layers. Specifically, consider a network defined as:

$$f_i^0(x) = \sum_j^I w_{ij}^0 x_j + b_i^0, \quad i = 1, \dots, H_0;$$

$$f^l(x) = \sum_j^{H_0} w_{ij}^l \phi(f_j^0(x)) + b^l$$

where  $x$  denotes the  $I$ -dimensional input, and  $f^l(x)$  represents the output at the  $l$ -th layer.

In a BNN,  $z_{ij}(x) = w_{ij}^l \phi(f_j^0(x))$  is a random variable. Assuming that the weights  $w_{ij}$  share a common prior and the biases  $b_i$  have independent but shared priors, the output  $f^l(x)$  becomes a sum of independent and identically distributed (i.i.d.) random variables. By the Central Limit Theorem, this results in  $f^l(x)$  converging to a Gaussian distribution, implying that the BNN

converges to a GP in the limit of infinite width.

The covariance between two inputs,  $x$  and  $x'$ , for the BNN at the (output) layer  $l$  is given by:

$$\text{Cov}(f^l(x), f^l(x')) = \sigma_b^l + \sigma_w^l \mathbb{E}_{f_j^0} [\phi(f_j^0(x)) \phi(f_j^0(x'))], \quad (1)$$

where  $\sigma_b^l$  and  $\sigma_w^l$  are respectively the variances of the biases and weights at layer  $l$  and the expectation is taken over distributions for  $w^0$  and  $b^0$ . Hence, the BNN functional prior corresponds to a GP with kernel  $\kappa_f^l(x, x') = \text{Cov}(f^l(x), f^l(x'))$ .

In this work, we assume zero-centered GPs. Therefore, for the distributions on weights and biases, we take  $\mathbb{E}[w] = 0$  and  $\mathbb{E}[b] = 0$ . To ensure that the variance remains stable as the layer width increases we scale  $\text{Var}[w_{ij}^l] = \frac{\sigma_w^l}{H_0}$ .

## 3 METHOD

### 3.1 Transfer of Priors from GPs to BNNs

Finding a GP equivalent to a pre-specified BNN can be easily done by a Monte Carlo estimate of Eq. 1. However, we focus on the more challenging inverse problem of imposing behavior akin to a  $\text{GP}(0, \kappa)$  on a BNN. The task is to identify appropriate priors on  $w^l$ ,  $b^l$ ,  $w^0$ ,  $b^0$ , and the activation  $\phi$  in Eq. 1 so that the covariance induced by the BNN aligns with the desired GP kernel  $\kappa$ . Ideally, we aim to have  $f^l \sim \text{GP}(0, \kappa)|_{\mathcal{X}}$ , meaning that the distribution of the BNN (pre-likelihood) outputs would closely match that of the GP across the input space  $\mathcal{X}$ , i.e.,  $p_{nn}(f^l(x)) = p_{gp}(f^l(x))$  for  $x \in \mathcal{X}$ .

In practice, however, we often settle for approximate matching over a finite index sets  $X \in \mathcal{X}$  (Shi et al., 2018; Sun et al., 2019), where the densities over BNN and GP outputs approximately align as  $p_{nn}(f^l(X)) \approx p_{gp}(f^l(X))$ . This matching is formulated as an optimization task:

$$p_{nn}^* = \underset{p_{nn}}{\text{argmin}} \frac{1}{S} \sum_{X \sim p_X} D(p_{nn}(f^l(X)), p_{gp}(f^l(X))),$$

where  $D$  is an *arbitrary* (but differentiable) divergence measure.

### 3.2 Differentiable Priors and Activations

The results presented in Section 2 hold for distributions with finite variances and light tails. In particular, we use basic zero-centered factorized Gaussians with learned variances, e.g.,  $p(w|\sigma_w^2)$  and  $p(b|\sigma_b^2)$ , as prior distributions on model weights and biases. To enable gradient-based optimization, such as gradient propagation through weight and bias samples, we reparameterize the distributions using the reparameterization

trick. Additionally, we propose to employ parametric and differentiable activations  $\phi(\cdot|\eta)$  to enhance the network’s flexibility. This allows us to incorporate complex functional priors within a single hidden layer of a BNN, even with simple prior distributions on weights and biases.

Given the reparameterized distributions on weights and biases, as well as parametric activations,  $p_{nn}$  is fully characterized by the parameters  $\lambda = \{\sigma_b^0, \sigma_w^0, \sigma_b^l, \sigma_w^l, \eta\}$ . The final optimization objective is then expressed as:

$$\lambda^* = \operatorname{argmin}_{\lambda} \frac{1}{S} \sum_{X \sim p_X} D(p_{nn}(f^l(X|\lambda)), p_{gp}(f^l(X))), \quad (2)$$

which is solved through gradient-based optimization with respect to  $\lambda$ . This formulation involves practical decisions regarding the divergence measure  $D$  and the choice of model for the activation function  $\phi$ .

The problem of learning activations for neural networks involves designing functions that enable networks to capture complex and non-linear relationships effectively. In principle, any function  $\phi : \mathcal{R} \rightarrow \mathcal{R}$  can serve as an activation, but the choice of  $\phi$  significantly impacts both the network’s expressiveness and its training dynamics. We explore several models for  $\phi$ , including Rational (Pade) activations (Molina et al., 2019), Piecewise Linear (PWL) activations<sup>1</sup>, and activations implemented as a neural network with a single narrow (with only 5 neurons) hidden layer, using ReLU/SiLU own activations. These functions are computationally efficient and introduce desirable non-linear properties, striking a balance between efficiency and the capacity to model intricate patterns.

### 3.3 Periodic Activations For Stationary GPs

The optimization in Eq. 2 acts on range of inputs  $X$ , where the BNN’s behavior increasingly resembles the GP as training progresses. However, there are no guarantees about the BNN’s behavior outside this subset, particularly far from it. This limitation is exacerbated by *local stationarity* in BNNs: although GPs with stationary kernels are *globally* stationary, BNNs usually only exhibit stationarity within a limited input range. Outside this range, the covariance induced by the BNN may diverge from the desired GP behavior. This localized training can cause uncertainty quantification issues. In regions far from the data, a BNN may either become overly confident or overly uncertain, depending on the priors and the mismatch between the BNN’s architecture and the GP’s true behavior. It is challenging to enforce global properties, like stationarity or smoothness, across the entire input space, as the BNN’s learned covariance structure is overly dependent

on the inputs’ range. To address this, we introduce trainable activations that are designed to exhibit periodic behavior. This approach is inspired by the result of Meronen et al. (2021), who showed that periodic activation functions induce stationarity in BNNs. The our proposed activations

$$\phi(x|\psi, A) = \sum_{i=1}^K A_i \cos(2\pi\psi_i x) + \sum_{j=1}^K A_j \sin(2\pi\psi_j x)$$

are inspired by Fourier analysis, with variational parameters  $\eta = \{\psi_i, A_i, \psi_j, A_j\}$ . We used  $K = 5$ .

### 3.4 Conditional Priors and Activations

We propose conditioning the priors on weights and biases, and activations in BNNs on the hyperparameters of a GP kernel, such as lengthscale. By incorporating GP hyperparameters directly into the BNN framework, we close the equivalence gap between GPs and BNNs, allowing BNNs to fully replicate the behavior of GPs. Previously, researchers were limited to fixing hyperparameters before training or employing workarounds like training with hierarchical kernels with hyperparameters sampled from hyperpriors (see, e.g., Tran et al. (2022)). In particular, the ability to include hyperparameters directly within BNNs enables marginal likelihood (evidence) optimization, facilitating effective model selection.

Although our work focuses on conditioning on GP hyperparameters, the proposed conditioning framework is however more general and could be extended to priors dependent on other factors, such as input data e.g., to enhance model robustness by allowing the BNN to adapt its priors based on the input range. This adaptation might alleviate issues with the locality of the matching BNN to a GP, as discussed in Section 3.3, and could make the trained functional priors more robust against data transformations.

We implemented conditioning using hypernetworks (Ha et al., 2017; Chauhan et al., 2024), as  $[\sigma, \eta] := \text{hnet}(\gamma|\theta)$ , where  $\sigma$  and  $\eta$  are the sets of parameters for the priors on weights and activations, respectively. Here,  $\gamma$  represents the set of conditioning hyperparameters, which are transformed by the hypernetwork  $\text{hnet}$ . The hypernetwork has its own parameters  $\theta$ , which are now optimized in Eq. 2 as  $\lambda = \{\theta\}$  instead of  $\{\sigma, \eta\}$ . For a fixed architecture of  $\text{hnet}$ ,  $\sigma$  and  $\eta$  are now fully determined by  $\gamma$  along with  $\theta$ .

### 3.5 Loss

The loss  $D$  measures the divergence between two distributions over functions. While  $p_{gp}$  can be sampled and evaluated (for fixed inputs GPs act like Gaussians),  $p_{nn}$  is implicitly defined by a BNN, meaning it can be

<sup>1</sup><https://pypi.org/project/torchpwl/>

sampled from, but not evaluated directly. Due to the implicit nature of  $p_{nn}$ ,  $D$  must be specified for samples  $\{f^l\}$  and approximated using Monte Carlo. This points towards KL-divergence from  $p_{nn}$  to  $p_{gp}$ . We however discovered that the standard losses fail for this task. For example, estimating the empirical entropy term ( $\int p_{nn}(f) \log(p_{nn}(f)) df$ ) for KL presents a numerical challenge. Consequently, we followed Tran et al. (2022) and relied on the Wasserstein distance instead:

$$\begin{aligned} D &= \left( \inf_{\gamma \in \Gamma(p_{nn}, p_{gp})} \int_{\mathcal{F} \times \mathcal{F}} d(f, f')^p \gamma(f, f') df df' \right)^{1/p} \\ &= \sup_{|\psi|_L \leq 1} \mathbb{E}_{p_{nn}}[\psi(f)] - \mathbb{E}_{p_{gp}}[\psi(f)] \end{aligned} \quad (3)$$

Unlike Tran et al. (2022), we used the 2-Wasserstein metric, which for Multivariate Gaussians (applicable in the case of GPs and wide BNNs, at least approximately) has a closed-form solution (Mallasto and Ferafen, 2017):

$$D = \|\mu_1 - \mu_2\|_2^2 + \text{Tr} \left( \Sigma_1 + \Sigma_2 - 2\sqrt{\sqrt{\Sigma_1} \Sigma_2 \sqrt{\Sigma_1}} \right),$$

where  $\mu_{1/2}$ ,  $\Sigma_{1/2}$  are respectively expectations and covariance matrices estimated for  $p_{nn}$  and  $p_{gp}$  from samples  $\{f^l(X)\}$  obtained at finite input sets  $X$ . Not only we avoid the internal optimisation due to  $\sup_{|\psi|}$ , but additionally  $D$  can be efficiently computed based on results by Buzuti and Thomaz (2023). For experiments, we report numerical values of  $D$  normalized by number of elements in  $X$ .

### 3.6 Output Structure

The optimization objective in Eq. 2 is defined over functions  $f$ , which are passed through likelihoods to form model outputs  $y$ , i.e., distributions over  $f$  determine distributions over  $y$ . For regression tasks, a Gaussian likelihood is typically used; for binary classification, Bernoulli; and for multiclass classification, a Categorical likelihood with  $f$  transformed via softmax. Note that the prior transfer is likelihood-independent, meaning it does not rely on how the latent functions  $f$  relate to the outputs  $y$ . Then, as explained in Section 3.5, the optimization can be performed efficiently between Gaussians. If these assumptions were not satisfied—e.g., if the desired priors are not expressible via a GP—we can revert to the nested optimization for  $|\psi|_L$  as implied by Eq. 3. Overall, we explain our method in terms of GPs and for brevity, we denote the target functional priors by  $p_{gp}$ . However, it is important to note that the method is applicable to *arbitrarily* specified functional priors.

For completeness, we follow to briefly discuss also the transfer of priors from GPs to BNNs for

multivariate/multi-class-output settings; however, adequate experiments are beyond the scope of this paper. In particular, the multivariate models (Rasmussen and Williams, 2005; Alvarez et al., 2012) can be approached using various architectural strategies, depending on the nature of the dependencies among the output dimensions. One approach is to construct independent BNNs for each output dimension, stacking them side-by-side, where each BNN is pretrained separately with priors obtained from independent single-output GPs. This approach is appropriate when output dimensions are assumed to be independent, leading to an ensemble of independently trained BNNs. Alternatively, a shared hidden layer BNN can be used, where a common hidden representation is shared across all output dimensions, thereby capturing potential dependencies between outputs. The shared hidden layer structure reflects the idea of a multi-output or multi-task GP, where dependencies among outputs can be modeled explicitly using coregionalization techniques (Goovaerts, 1997; Bonilla et al., 2008). The shared hidden layer BNN can thus be endowed with priors derived from these multi-output GPs, ensuring that both spatial and output correlations are incorporated into the BNN model.

### 3.7 Optimisation Challenges

The problem of finding BNNs behaving like GPs (e.g. inverting covariance equation) is unidentifiable. There exist multiple solutions assuring similar quality of the final match. In particular, activations  $\phi$  solving Eq.(2) are not unique:

- The solutions are symmetric w.r.t activity values (y-axis), i.e., for  $\phi'(f) = -\phi(f)$ , values of covariance given by Eq.(1) are not changed, simply because  $(-1)^2 = 1$ .
- For  $p(f_i^0(x))$  symmetric around 0 (for example, Gaussians), activations with flipped arguments  $\phi'(f) = \phi(-f)$  result in the same covariances.
- Scaling activations  $\phi'(f) = \alpha\phi(f)$  leads to the same covariances as scaling variances of the output weights as  $(\sigma_w^l)' = \alpha \cdot \sigma_w^l$

Given a sufficiently flexible model (like a neural network itself), one can learn to approximate any target activation function to an arbitrary degree of accuracy on a compact domain. This is in line with the universal approximation theorem. However, in practice there are multiple limitations and challenges. A model may require an impractically large number of parameters to approximate certain complex functions to a desired level of accuracy. More complex models may be harder to fit and may require more training data. Some functions might require high numerical precision to be approximated effectively, and even if a model can fit a target activation function on a compact set, it might not generalize well outside the training do-

main. Overall, there are multiple factors that may lead gradient-based optimization to fail for our task. Such the outcome however will be reflected in poor values of the final loss (Eq. 3). A practical remedy would be then rerunning the optimisation, once poorly performing outliers were noticed.

## 4 EMPIRICAL RESULTS

To present the capabilities and effectiveness of using learnable activations while matching BNNs to GPs, we perform a wide set of experiments comparing our approach against the most canonical methods for transferring GPs into BNNs (e.g., by Meronen et al. (2020) and Tran et al. (2022)).

We structure this section as follows: first we ask a specific question, and then, respond to it, based on empirical results.

For a detailed description of the experimental settings and additional results, please see Appendix.

### 4.1 Can Learned Activations Achieve More Faithful Function-space Priors?

To map GP function-space priors to a BNN, we can: 1) train its priors on parameters, 2) train both priors and activation, or 3) learn just the activation function. We empirically show that learning also activations provide better solutions to the inverse problem of imposing function-space priors on BNNs.

Figure 1 illustrates the results of an extensive study where we compare the quality of the GP prior fit for various models of parameters’ priors and activations. The target was  $GP(0, \text{Matern}(\nu = 5/2, \ell = 1))$ . For each configuration, we conducted several training iterations and measured the final (converged) loss value multiple times.

Generally, learning activations alone is not sufficient for good fits, but when combined with learning priors, it significantly improves the results.

### 4.2 Do Expressive Function-space Priors Require Networks to be Deep?

Expressive function-space priors require a flexible and expressive BNN model, which can be achieved either through a deep architecture or by a shallow BNN but with more flexible (e.g., learnable) activations. Until now, only the first approach has been explored.

For instance, Tran et al. (2022) takes a practical approach to learning function-space priors by focusing on deep networks. Rather than considering BNNs with wide layers, for which the theoretical results in Section 2 hold, they *postulate* that a deep network as a whole can model a functional prior. They then

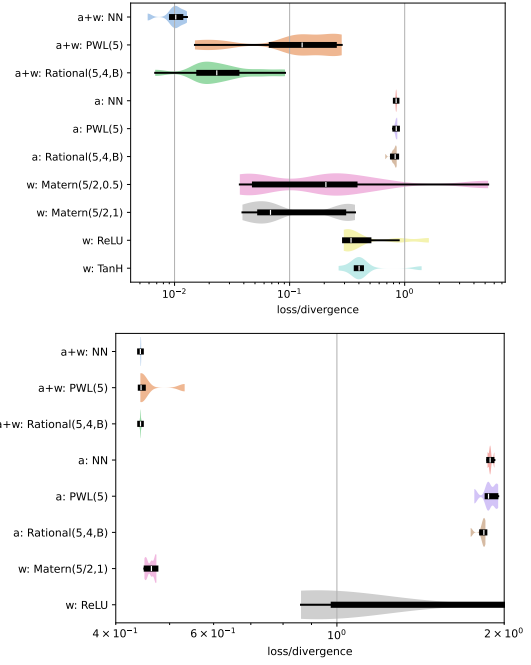


Figure 1: Quality of matching BNNs to the prior of a GP with a Matern kernel ( $\nu = 5/2, \ell = 1$ ) for 1D (top) and 16D inputs (bottom). We evaluate models with trained parameter priors (denoted by  $w$ ), activations (denoted by  $a$ ), and both (denoted by  $a+w$ ). Each label specifies whether a fixed activation (e.g., ReLU) or a specific activation model (e.g., Rational) was employed. Gaussian parameter priors were used by default. If not trained, we set variances to 1., and for the hidden layer, we normalized the variance by its width. The label  $w: \text{Matern}$  refers to a BNN with the closed-form (fixed) activation as derived by Meronen et al. (2020).

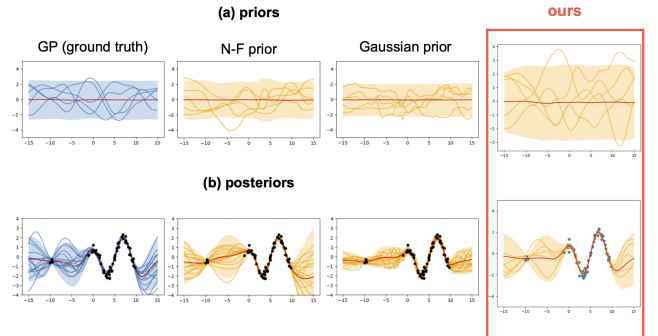


Figure 2: Prior (a) and posterior (b) predictive distributions for a BNN with trained parameters priors and activations (ours; 4th column), and for Tran et al. (2022) approach with different prior realizations (Gaussian - 3rd column and Normalizing Flow - 2nd). The first column illustrates the ground truth (GP). Numerical results complementing the figures we provide in Appendix.

Table 1: Results for UCI regression task (Boston dataset) with prior transferred from a GP; comparison between the baseline (using a deep BNN; (Tran et al., 2022)) and ours (single hidden layer BNN with varying widths). *Periodic activation* (Sec. 3.3) and an activation realized by a NN with SiLU own activation (*default*) were used.

Method →	our (width = 128, periodic act.)		our (width = 128)		our (width = 1000)		Baseline
Metric ↓	- regularization	+ regularization	- regularization	+ regularization	- regularization	+ regularization	—
RMSE	2.9067±0.8257	2.8967±0.8258	2.8643±0.8386	<b>2.8348±0.8371</b>	2.9189±0.8408	3.0059±0.9068	2.8402±0.8986
NLL	2.5057±0.1870	2.5072±0.1904	2.4937±0.1798	2.4862±0.1763	2.5122±0.1871	2.5971±0.1206	<b>2.4778±0.1481</b>

tune the network’s parameters to match a target prior. This however involves modeling complex priors across all weights jointly, using techniques like Normalizing Flows (Rezende and Mohamed, 2015) to achieve sufficient fidelity. This also introduces additional challenges in posterior inference for deep networks: MCMC algorithms (Chen et al., 2014; Del Moral et al., 2006) become computationally expensive and approximate methods (Hoffman et al., 2013; Ritter et al., 2018) lack the expressiveness needed to accurately handle such complex priors.

We propose an alternative approach and demonstrate that a BNN with a single wide hidden layer, basic Gaussian priors, and learned activations can match or even outperform the results of Tran et al. (2022), in terms of both priors and posteriors quality. We compare this approach against (Tran et al., 2022) on a set of regression problems – both artificial and real ones (Boston dataset from UCI). The results are presented in Fig. 2 and in Tab. 1 respectively. We closely followed the settings by Tran et al. (2022).

Moreover, we check the findings from (Wu et al., 2024) that moment matching helps biasing optimisation towards better solutions. In the UCI regression task, we include an additional moment matching regularization term:  $\mathcal{R}(p_{nn}, p_{gp}) = (\mathbb{E}_{p_{nn}}[var(f)] - \mathbb{E}_{p_{gp}}[var(f)])^2 + (\mathbb{E}_{p_{nn}}[kurtosis(f)] - \mathbb{E}_{p_{gp}}[kurtosis(f)])^2 + (\mathbb{E}_{p_{nn}}[skewness(f)] - \mathbb{E}_{p_{gp}}[skewness(f)])^2$ . However, we haven’t observed any significant trend if this regularization helps or not.

Additional results for remaining UCI regression tasks we provide in Appendix.

### 4.3 Can Learned Activations Match Performance of the Closed-form Ones?

Complexity of deriving suitable neural activations makes matching BNNs to GPs a formidable challenge. We instead propose a gradient-based learning method that adapts both activation and parameters priors. This approach departs from the traditional methods that rely on fixed, analytically derived activations, offering instead a flexible alternative that empirically can match or even surpass the performance of the more conventional approaches.

The empirical evaluation we performed for a problem of

2D data classification following Meronen et al. (2020), with a GP, where the authors derived analytical activation to match the Matern kernel exactly. For our method, we used a BNN with Gaussian priors with trained variances, where the activation function was modeled by a NN with a single hidden layer consisting of 5 neurons using SiLU activation. Posterior distributions were generally obtained using a HMC sampler.

The results presented in Fig. 3 (and numerical results provided in Appendix) demonstrate that our method enhances the match between the posteriors of a BNN and the desired target GP. Note that Meronen et al. (2020) originally used MC Dropout to obtain the posteriors, achieving much worse results than those obtained with HMC. For fairness in comparison, we tested both MC Dropout and HMC. In terms of performance, our model not only captures class probabilities accurately but also adeptly handles the total variance in class predictions and the epistemic uncertainty component, which are crucial for robust decision-making under uncertainty.

### 4.4 Can Stationarity be Induced with Learned Periodic Activations?

Trained priors for BNNs are inherently local, effectively mimicking GP behavior only within the range of training inputs  $X$ . As illustrated in Fig. 4 (top), outside this range, the BNN’s learned prior may diverge from the desired behavior, and properties such as stationarity or smoothness may not be preserved beyond the observed input domain. We however can not only detect this issue by noting high values of the divergence, but also mitigate it by using activations with appropriate structural biases. Specifically, the periodic activation introduced in Section 3.3 proves to be robust to input domain translations, as demonstrated in Fig. 4 (bottom).

### 4.5 Is Model Selection for BNNs with Transferred Priors Possible?

A BNN with a functional prior learned from a GP essentially inherits the properties dictated by the GP, including those determined by specific values of the GP’s hyperparameters. While the hyperparameters of the source GP can be tuned and optimized, the BNN does not inherently possess this capability, requiring researchers to either pre-optimize the hyperparameters or

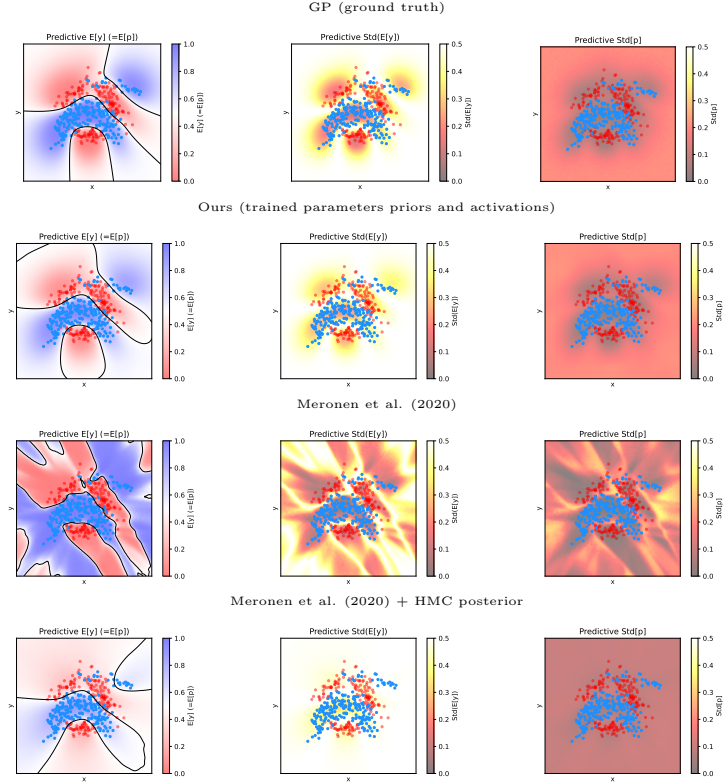


Figure 3: Posterior predictive distributions for a BNN with trained parameters priors and activations (ours; 2nd row), and for a BNN with analytically derived activation (3rd and 4th row). The first column illustrates class probabilities, the second column shows the total variance in class predictions, and the last column depicts the epistemic uncertainty component of the total uncertainty. Numerical results complementing the figures we provide in Appendix.

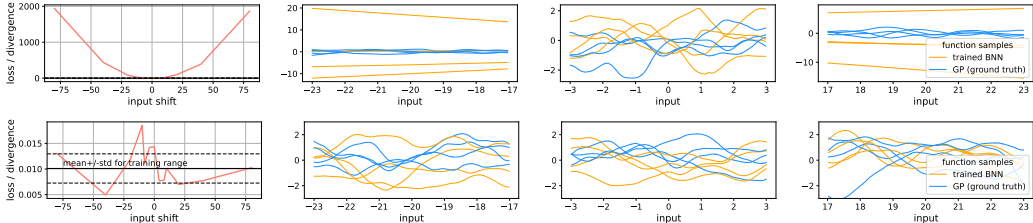


Figure 4: Sensitivity of priors transferred from a GP to a BNN with respect to shifts in the input range for learned activations: (top) activation realized by a NN with a single hidden layer containing 5 neurons and SiLU own activation; (bottom) periodic activation introduced in Section 3.3. Priors were trained on random inputs  $X \in [-3, 3]$ . The first column shows the mismatch between the desired target GP and the trained BNN prior for shifted input ranges, measured by the 2-Wasserstein loss. The remaining columns present samples from the priors for three ranges: one matching the training range and two far from it.

look for suitable workarounds (Tran et al., 2022). Conditioning the priors on weights, biases, and activation, as explained in Section 3.4, addresses this limitation. Figure 5 shows results for a prior trained to adapt to a varying lengthscale of a Matern kernel. The prior closely follows the behavior of the ground truth model.

To validate the usefulness of this method, we performed marginal likelihood maximization on the data from Figure 2, using gradient-based optimization for both the GP with the Matern kernel and our BNN. The

optimal lengthscale found for the BNN ( $\ell = 1.65$ ) closely matches the one found for the GP ( $\ell = 1.84$ ).

## 5 RELATED WORK

The relationship between (B)NNs and GPs has been a subject of significant research interest. Much of this work has been motivated by the desire to better understand NNs through their connection to GPs. A seminal result by Neal (1996); Williams (1996), later extended to deep NNs by Lee et al. (2017) and Matthews et al.

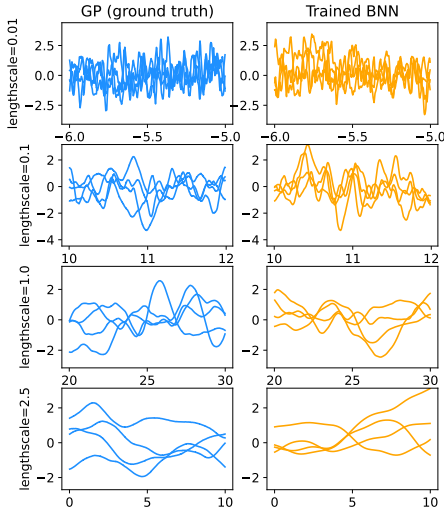


Figure 5: Comparison of samples from a GP (left) and a trained BNN (right) using priors and activations (periodic activation as in Section 3.3) conditioned on the GP’s hyperparameters (e.g., lengthscale). The BNN was trained on random inputs  $X \in [-3, 3]$ . Regardless of input range and the hyperparameter’s value, the samples from both models appear indistinguishable.

(2018), shows that infinitely wide layers in NNs exhibit behavior akin to GPs. While we explore a similar setting, our focus is the inverse: implementing function-space priors, specifically GP-like, within BNNs.

This problem was previously addressed by Meronen et al. (2020), who proposed an activation function for BNNs that corresponds to the popular Matern kernel. Due to the complexity of deriving analytical solutions, other works, such as Flam-Shepherd et al. (2017, 2018); Tran et al. (2022), have explored gradient-based optimization to learn priors on weights and biases. However, their approach requires deep networks with complex distributions and additionally, presents a challenge in learning posterior. In contrast, we achieve high-fidelity functional priors in shallow BNNs by matching *both* priors on parameters and activations.

Finding accurate posteriors for deep and complex models such as BNNs is notoriously challenging due to their high-dimensional parameter spaces and complex likelihood surfaces. However, for single-hidden-layer wide BNNs, it has been recently shown that posterior sampling via Markov Chain Monte Carlo can be performed efficiently (Hron et al., 2022). Moreover, research has demonstrated that the exact posterior of a wide BNN weakly converges to the posterior corresponding to the GP that matches the BNN’s prior (Hron et al., 2020). This allows BNNs to inherit GP-like properties while preserving their advantages.

An alternative line of work touching efficient learning for BNNs in function space has explored variational inference. Sun et al. (2019) introduced functional vari-

ational BNNs (fBNNs) that maximize an Evidence Lower Bound defined over functions. However, Burt et al. (2020) highlighted issues with using the Kullback-Leibler divergence in function space, leading to ill-defined objectives. To overcome this, methods like Gaussian Wasserstein inference (Wild et al., 2022) and Functional Wasserstein Bridge Inference (Wu et al., 2024) leverage the Wasserstein distance to define well-behaved variational objectives. These approaches try to incorporate functional priors into variational objective for deep networks. In contrast, in our method transfer of priors to shallow BNNs remains independent and fully separated from an inference method.

Finally, other works worth mentioning include Meronen et al. (2021), who explored periodic activation functions in BNNs to connect network weight priors with translation-invariant GP priors. Pearce et al. (2020) derived BNN architectures to mirror GP kernel combinations, showcasing how BNNs can produce periodic kernels. Karaletsos and Bui (2020) introduced a hierarchical model using GP for weights to encode correlated weight structures and input-dependent weight priors, aimed at regularizing the function space. Matsubara et al. (2021) proposed using ridgelet transforms to approximate GP function-space distributions with BNN weight-space distributions, providing a non-asymptotic analysis with finite sample-size error bounds. Finally, Tsuchida et al. (2019) extended the convergence of NN function distributions to GPs under broader conditions, including partially exchangeable priors. A more detailed discussion of related topics can be found for example, in Sections 2.3 and 4.2 of (Fortuin, 2022).

## 6 CONCLUSION

In this paper, we addressed the problem of transferring functional priors for wide Bayesian Neural Networks to replicate desired a priori properties of Gaussian Processes. Previous approaches typically focused on learning distributions over weights and biases, often requiring deep BNNs for sufficient flexibility. We proposed an alternative approach by also learning activations, providing greater adaptability even for shallow models and eradicating the need for task-specific architectural designs. To the best of our knowledge, we are the first to explore learning activations in this context. Moreover, to further enhance adaptability of these transferred priors, we came up with the idea of conditioning them with hypernetworks, which opens a new interesting future research direction. To demonstrate the flexibility and effectiveness of the proposed methods, we conducted a comprehensive experimental study validating our ideas.

**Future Work** In the future, we plan to extend the proposed method to be used as plug-and-play last layer and also to consider transfer from multivariate GPs.

## Acknowledgements

This research is part of the project No. **2022/45/P/ST6/02969** co-funded by the National Science Centre and the European Union Framework Programme for Research and Innovation Horizon 2020 under the Marie Skłodowska-Curie grant agreement No. 945339. For the purpose of Open Access, the author has applied a CC-BY public copyright licence to any Author Accepted Manuscript (AAM) version arising from this submission.



This research was in part funded by National Science Centre, Poland, **2022/45/N/ST6/03374**.

We gratefully acknowledge Polish high-performance computing infrastructure PLGrid (HPC Center: ACK Cyfronet AGH) for providing computer facilities and support within computational grant no. **PLG/2023/016302**.

## References

Alvarez, M. A., Rosasco, L., and Lawrence, N. D. (2012). Kernels for vector-valued functions: A review. *Foundations and Trends® in Machine Learning*, 4(3):195–266.

Bonilla, E. V., Chai, Y., and Williams, C. K. (2008). Multi-task gaussian process prediction. In *Advances in Neural Information Processing Systems*, pages 153–160.

Burt, D. R., Ober, S. W., Garriga-Alonso, A., and van der Wilk, M. (2020). Understanding variational inference in function-space. *Third Symposium on Advances in Approximate Bayesian Inference*.

Buzuti, L. F. and Thomaz, C. E. (2023). Fréchet autoencoder distance: a new approach for evaluation of generative adversarial networks. *Computer Vision and Image Understanding*, 235:103768.

Chauhan, V. K., Zhou, J., Lu, P., Molaei, S., and Clifton, D. A. (2024). A brief review of hypernetworks in deep learning. *Artificial Intelligence Review*, 57(9):1–29.

Chen, T., Fox, E., and Guestrin, C. (2014). Stochastic gradient hamiltonian monte carlo. In *International conference on machine learning*, pages 1683–1691. PMLR.

Del Moral, P., Doucet, A., and Jasra, A. (2006). Sequential Monte Carlo Samplers. *Journal of the Royal Statistical Society Series B: Statistical Methodology*, 68(3):411–436.

Flam-Shepherd, D., Requeima, J., and Duvenaud, D. (2017). Mapping gaussian process priors to bayesian neural networks. In *NIPS Bayesian deep learning workshop*, volume 3.

Flam-Shepherd, D., Requeima, J., and Duvenaud, D. (2018). Characterizing and warping the function space of bayesian neural networks. In *NeurIPS Workshop on Bayesian Deep Learning*, page 18.

Fortuin, V. (2022). Priors in bayesian deep learning: A review. *International Statistical Review*, 90(3):563–591.

Goovaerts, P. (1997). Geostatistics for natural resources evaluation.

Ha, D., Dai, A., and Le, Q. V. (2017). Hypernetworks. In *ICLR. International Conference on Representation Learning*.

Hoffman, M. D., Blei, D. M., Wang, C., and Paisley, J. W. (2013). Stochastic variational inference. *Journal of Machine Learning Research (JMLR)*, 14:1303–1347.

Hron, J., Bahri, Y., Novak, R., Pennington, J., and Sohl-Dickstein, J. (2020). Exact posterior distributions of wide bayesian neural networks. *arXiv preprint arXiv:2006.10541*.

Hron, J., Novak, R., Pennington, J., and Sohl-Dickstein, J. (2022). Wide Bayesian neural networks have a simple weight posterior: theory and accelerated sampling. In Chaudhuri, K., Jegelka, S., Song, L., Szepesvari, C., Niu, G., and Sabato, S., editors, *Proceedings of the 39th International Conference on Machine Learning*, volume 162 of *Proceedings of Machine Learning Research*, pages 8926–8945. PMLR.

Karaletsos, T. and Bui, T. D. (2020). Hierarchical gaussian process priors for bayesian neural network weights. *Advances in Neural Information Processing Systems*, 33:17141–17152.

Lee, J., Bahri, Y., Novak, R., Schoenholz, S. S., Pennington, J., and Sohl-Dickstein, J. (2017). Deep neural networks as gaussian processes. *arXiv preprint arXiv:1711.00165*.

Mallasto, A. and Feragen, A. (2017). Learning from uncertain curves: The 2-wasserstein metric for gaussian processes. In Guyon, I., Luxburg, U. V., Bengio, S., Wallach, H., Fergus, R., Vishwanathan, S., and Garnett, R., editors, *Advances in Neural Information Processing Systems*, volume 30. Curran Associates, Inc.

Matsubara, T., Oates, C. J., and Briol, F.-X. (2021). The ridgelet prior: A covariance function approach to prior specification for bayesian neural networks. *The*

*Journal of Machine Learning Research*, 22(1):7045–7101.

Matthews, A. G. d. G., Rowland, M., Hron, J., Turner, R. E., and Ghahramani, Z. (2018). Gaussian process behaviour in wide deep neural networks. *ICLR*.

Meronen, L., Irwanto, C., and Solin, A. (2020). Stationary activations for uncertainty calibration in deep learning. *Advances in Neural Information Processing Systems*, 33:2338–2350.

Meronen, L., Trapp, M., and Solin, A. (2021). Periodic activation functions induce stationarity. *Advances in Neural Information Processing Systems*, 34:1673–1685.

Molina, A., Schramowski, P., and Kersting, K. (2019). Padé activation units: End-to-end learning of flexible activation functions in deep networks.

Neal, R. M. (1996). *Bayesian Learning for Neural Networks*, Vol. 118 of *Lecture Notes in Statistics*.

Pearce, T., Tsuchida, R., Zaki, M., Brintrup, A., and Neely, A. (2020). Expressive priors in bayesian neural networks: Kernel combinations and periodic functions. In *Uncertainty in artificial intelligence*, pages 134–144. PMLR.

Qiu, S., Rudner, T. G. J., Kapoor, S., and Wilson, A. G. (2024). Should we learn most likely functions or parameters? In *Proceedings of the 37th International Conference on Neural Information Processing Systems*, NIPS ’23, Red Hook, NY, USA. Curran Associates Inc.

Rasmussen, C. E. and Williams, C. K. I. (2005). *Gaussian Processes for Machine Learning (Adaptive Computation and Machine Learning)*. The MIT Press.

Rezende, D. and Mohamed, S. (2015). Variational inference with normalizing flows. *International Conference on Machine Learning (ICML)*.

Ritter, H., Botev, A., and Barber, D. (2018). A scalable laplace approximation for neural networks. In *6th international conference on learning representations, ICLR 2018-conference track proceedings*, volume 6. International Conference on Representation Learning.

Shi, J., Sun, S., and Zhu, J. (2018). A spectral approach to gradient estimation for implicit distributions. In *International Conference on Machine Learning*, pages 4644–4653. PMLR.

Sun, S., Zhang, G., Shi, J., and Grosse, R. (2019). Functional variational bayesian neural networks. In *Advances in Neural Information Processing Systems*, volume 32, pages 5690–5701.

Tran, B.-H., Rossi, S., Milios, D., and Filippone, M. (2022). All you need is a good functional prior for bayesian deep learning. *Journal of Machine Learning Research*, 23(74):1–56.

Tsuchida, R., Roosta, F., and Gallagher, M. (2019). Richer priors for infinitely wide multi-layer perceptrons. *arXiv preprint arXiv:1911.12927*.

Wild, V. D., Hu, R., and Sejdinovic, D. (2022). Generalized variational inference in function spaces: Gaussian measures meet bayesian deep learning. *Advances in Neural Information Processing Systems*, 35:3716–3730.

Williams, C. (1996). Computing with infinite networks. In Mozer, M., Jordan, M., and Petsche, T., editors, *Advances in Neural Information Processing Systems*, volume 9. MIT Press.

Wu, M., Xuan, J., and Lu, J. (2024). Functional wasserstein bridge inference for bayesian deep learning. In *The 40th Conference on Uncertainty in Artificial Intelligence*.

We supplement here the main paper with details of the experimental setting followed by additional numerical results.

## A Code

Code is available at <https://github.com/gmum/bnn-functional-priors> and will continue to be maintained and extended.

## B Experimental Setting

### B.1 1-dimensional Regression - Comparison with Tran et al. (2022)

In order to illustrate the abilities of our approach on a standard regression task and for a fair comparison with another method optimizing the Wasserstein distance, we followed the exact experimental setting presented in Tran et al. (2022). We used a GP with an RBF kernel (*length scale*  $\ell=0.6$ , *amplitude*=1.0) and a Gaussian likelihood (*noise variance*=0.1) as the ground truth.

For a baseline, we utilized the approach by Tran et al. (2022), consisting of a BNN with 3 layers and 50 neurons each, using TanH activation function. We considered all three prior realizations presented in that work: a simple Gaussian prior, a hierarchical prior, and a prior given by a Normalizing Flow. On the other hand, our model configuration consisted of a BNN with Gaussian priors centered at **0** and trained variances, where the activation function was modeled by a neural network with a single hidden layer with 5 neurons and SiLU activation. Posterior distributions were obtained using an HMC sampler.

We found that our approach allows for achieving the same or better results than the baseline by Tran et al. (2022), both in visual and numerical comparisons. We obtained better results in terms of distributional metrics as presented in Tab. 3 and getting better (visually) posterior distributions (see Fig. 2) without utilizing any computationally heavy prior realization (like, e.g., Normalizing Flow).

### B.2 UCI regression - Comparison with Tran et al. (2022)

In addition, we compare against Tran et al. (2022) also on UCI regression tasks, which have more input dimensions  $d$  – between 8 and 12, while having 1-dimensional output. We use 10-split of training datasets as is typical in this direction of research.

For the baseline, we followed the exact experimental setting presented in Tran et al. (2022). We used a GP with an RBF kernel (*length scale*  $\ell = \sqrt{2.0 * \text{input\_dim}}$  and *amplitude*=1.0, *ARD*) and a Gaussian likelihood as the ground truth. We set the noise variance value and architectures for the specific datasets as in the mentioned baseline paper.

On the other hand, our model configuration consisted of a BNN with Gaussian priors centered at **0** and trained variances, where the activation function was modeled by a neural network with a single hidden layer with 5 neurons and SiLU activation. Posterior distributions were obtained using an HMC sampler.

We found that our approach allows for achieving the same or better results than the baseline, in terms of numerical values (*RMSE* and *NLL*) as presented in Tab. 2.

Table 2: Extended results for a set of UCI regression tasks (various input dimensionality  $d$ ) with prior transferred from a GP; comparison between the baseline (using a deep BNN; (Tran et al., 2022)) and ours (single hidden layer BNN with 128 neurons; w/o regularization) and an activation realized by a NN with SiLU own activation were used.

Dataset →	Boston ( $d = 12$ )		Concrete ( $d = 8$ )		Energy ( $d = 8$ )		Protein ( $d = 9$ )		Wine ( $d = 11$ )		
	Method ↓ Metric →	RMSE	NLL	RMSE	NLL	RMSE	NLL	RMSE	NLL	RMSE	NLL
baseline		2.8402±0.8986	2.4778±0.1481	4.4628±0.7511	2.9728±0.0876	0.3431±0.0613	0.3482±0.1607	0.5038±0.0093	0.7447±0.0142	0.4736±0.0420	0.8725±0.0285
ours		2.8643±0.8386	2.4937±0.1798	4.9143±0.7528	3.0201±0.1011	0.3692±0.0566	0.4064±0.1347	0.4957±0.0058	0.7251±0.0094	0.4833±0.0398	0.8673±0.0255

### B.3 Classification - Comparison with Meronen et al. (2020)

For the comparison against Meronen et al. (2020), we closely followed their experimental setting and used a GP with a Matern kernel ( $\nu = 5/2$ ,  $\ell=1$ ) as the ground truth. For a baseline, we utilized the approach by Meronen et al. (2020), where the authors derived analytical activations to match the Matérn kernel. Our model configuration consists of a BNN with Gaussian priors and trained variances, where the activation function was modeled by a neural network with a single hidden layer consisting of 5 neurons using SiLU activation. Posterior distributions were generally obtained using an HMC sampler, except in the case of Meronen et al. (2020), where the original implementation employed MC Dropout to approximate the posterior. However, for completeness and fairness in comparison, we also generated results using an HMC-derived posterior for the model by Meronen et al. (2020). Additional tests (see Tab. 4) were conducted on BNNs with fixed parameter priors (*Default*=Gaussian priors with a variance of 1, and *Normal*=Gaussian priors normalized by the hidden layer width) and with activation functions including ReLU and TanH.

### B.4 Periodic and Conditional Activations

BNNs with periodic activations were trained on functions sampled from a GP with a Matern kernel with  $\nu = \frac{5}{2}$  and length scales  $\ell$  of magnitudes ranging from 0.01 to 10.0. The inputs were randomly sampled from the interval  $[-3\ell, 3\ell]$ . Each input batch comprised 8 sets  $X$ , each containing 512 values  $x$ . For each set, 128 functions were sampled. Adam optimizer, with a learning rate of 0.01, was employed over 4000 iterations.

For the conditioning of priors and activations, a MLP hypernetwork was utilized. This hypernetwork consisted of 3 hidden layers with respective widths of 128, 32, and 8, and RBF activations. On top of the hidden layers, separate dense heads were deployed for each output—a 4-dimensional head for producing variances and two 10-dimensional heads for generating  $\{\psi\}$  and  $\{A\}$ . Each head projected the output of the last hidden layer to the requested dimensions.

## C Additional Numerical Evaluation

In this section, we present the comprehensive numerical evaluation for the experiments from the main paper. The results for regression experiments are presented in Tab. 3, whereas the results for classification are presented in Tab. 4.

Table 3: Comparison between (Tran et al., 2022) and our method of the similarity of trained (function-space) priors and posteriors in a 1D regression task. Whereas Tran et al. (2022) considered three different priors on parameters (including Gaussian, Hierarchical, and Normalizing Flow) for deep BNNs, our implementation consists of a single-hidden-layer BNN with standard Gaussian priors with learned variances and trained activation. The methods were compared using a set of distributional metrics against the ground truth provided by a GP (following the code by Tran et al. (2022)). We compared both prior and posterior predictive distributions of functions over a range of  $X$  covering regions with and without data (to account also for overconfidence far from data). The lower, the better.

Setting	RMSE	NLL	1-Wasserstein	2-Wasserstein	Linear-MMD	Poly-MMD $\times 10^3$	RBF-MMD	Mean-MSE	Mean-L2	Mean-L1	Median-MSE	Median-L2	Median-L1
<b>Priors:</b>													
Gaussian prior	—	—	7.49	7.55	-3.48	1.225	0.033	0.003	0.055	0.048	0.007	0.084	0.070
Hierarchical prior	—	—	8.14	8.37	0.22	1.421	0.027	0.004	0.064	0.059	0.008	0.090	0.074
Normalizing Flow prior	—	—	7.76	8.16	-2.36	0.388	0.021	0.005	0.071	0.057	0.006	0.076	0.057
<b>ours</b>	—	—	7.02	7.21	-8.68	0.088	0.008	0.004	0.062	0.053	0.007	0.086	0.074
<b>Posteriors:</b>													
Gaussian prior	0.2862	0.2885	6.59	6.78	23.45	5.272	0.26	0.259	0.509	0.332	0.294	0.542	0.354
Hierarchical prior	0.2461	0.2613	5.61	5.84	15.12	3.1	0.153	0.112	0.335	0.216	0.122	0.349	0.219
Normalizing Flow prior	0.2585	0.2518	6.81	7.00	34.19	7.044	0.263	0.275	0.524	0.383	0.368	0.607	0.423
<b>ours</b>	0.3086	0.3280	10.76	10.91	78.66	8.133	0.739	0.781	0.883	0.703	0.794	0.891	0.713

Table 4: Similarity of the posterior predictive distributions of BNNs with a single wide hidden layer to the posterior of a GP, considered as ground truth. Calculations were performed for a test grid that includes regions both with and without training data to account for overconfidence far from data. The posteriors were obtained using the HMC sampler in all cases, except for (Meronen et al., 2020), where the original code was used (however, results for this model with a HMC-derived posterior are also included below). The lower, the better. For our method, we present results using weights and priors pretrained for 1D inputs, as well as those trained on functional priors for 1D/2D inputs matched to the task on  $X$  (see Fig. 3).

Setting	1-Wasserstein	2-Wasserstein	Linear-MMD	Mean-L1	Mean-L2	Mean-MSE	Median-L1	Median-L2	Median-MSE	Poly-MMD $\times 10^3$	RBF-MMD
Default with ReLU	39	39	667	0.23	0.26	0.067	0.3	0.33	0.11	4518	0.16
Default with TanH	38	38	595	0.22	0.24	0.058	0.3	0.32	0.11	4181	0.15
Normal with ReLU	31	32	603	0.21	0.25	0.061	0.22	0.26	0.069	3093	0.47
Normal with TanH	25	25	314	0.14	0.18	0.031	0.15	0.18	0.034	1721	0.55
(Meronen et al., 2020)	36	36	777	0.24	0.28	0.078	0.28	0.32	0.1	7311	0.24
Normal + HMC	21	21	72	0.07	0.09	0.007	0.071	0.094	0.009	435	0.24
Default + HMC	42	42	284	0.14	0.16	0.026	0.32	0.34	0.12	1867	0.11
<b>Ours: pretrained 1D</b>	25	25	73	0.06	0.09	0.008	0.076	0.1	0.011	771	0.07
<b>Ours: trained 1D</b>	23	23	6	0.03	0.03	0.001	0.029	0.035	0.001	45	0.03
<b>Ours: trained 2D</b>	23	23	13	0.03	0.03	0.001	0.028	0.035	0.001	74	0.02